Probabilistic Fuzzy Multi-Objective Optimal Power Flow

Prakaipetch Muangkhiew[1] and Keerati Chayakulkheeree[1,*]

ARTICLE INFO

Article history:
Received: 08 October 2022
Revised: 12 December 2022
Accepted: 29 January 2023

Keywords:
Multi-objective optimization
Probabilistic optimization
Probabilistic density function
Optimal power flow

ABSTRACT

This study presents a probabilistic fuzzy multi-objective optimal power flow (PFMOPF) method that accounts for the generation of photovoltaic and wind power plants (PVPP and WPP) as well as load uncertainty. This method uses probabilistic models to predict the power output of PVPP and WPP generation associated with wind speed and solar irradiance data. The optimal power flow (OPF) formulation treats the active power of PVPP and WPP as dependent variables while handling the voltage magnitudes of PVPP and WPP generator buses as control variables. Additionally, the method incorporates several objective functions, including voltage magnitude deviation minimization (VMDM), active power loss minimization (APLM), and total system cost minimization (TSCM). Moreover, a fuzzy satisfaction function for the objectives is obtained by particle swarm optimization (PSO), which solves the multi-objective coordination issue. With the addition of PVPP and WPP, the proposed PFMOPF method is assessed using the adjusted IEEE 30-bus system, along with Monte Carlo simulation (MCS). Considering the PVPP, WPP, and load uncertainty of the system, this technique succeeds in adjusting the satisfaction function for multi-objective optimal power flow. The suggested strategy offers probabilistic values for the best variables. Ultimately, as a result, the total system cost, the active power loss, the voltage magnitude deviation, and λ_T (a parameter utilized in the PFMOPF) are found to be 535.123 $/h, 2.523 p.u., 0.429 p.u., and 0.741, respectively.

NOMENCLATURES

σ = load demand standard deviation.
$|\tilde{V}_{Gi}|$ = generator i voltage magnitude.
$|\tilde{V}_i|$ = bus i voltage magnitudes.
$|\tilde{V}_i^{ref}|$ = bus i reference value voltage magnitude.
$|\tilde{V}_{Li}|$ = load bus i voltage magnitude.
μ = load demand mean value.
a_i, b_i, c_i = generator i cost function parameters.
APL, APL_{max} , APL_{min} = real power loss and its maximum and minimum value.
B_{ij} = line i - j susceptance.
c = Weibull scale parameter.
$f_G(G)$ = solar irradiance.
F_i = objective function.
$f_{Pd}(P_d)$ = load demand.
$f_v(v)$ = wind speed Weibull.
$\boldsymbol{g}$ = equality constraints.
G_{ij} = line i - j conductance.
h = system operation constraints.
k = Weibull shape parameter.
$M\tilde{V}A_{Li}$ = line i appearance power flow.
NB, NC, NG, NL, N_{obj}, NPQ, NT, NTL = number of buses, shunt compensators, generators, branches, objectives, PQ buses, transformers, and transmission line.
$\tilde{P}_{Di}$, $\tilde{P}_{Gi}$ = bus i real power demand and generation.
$\tilde{P}_{pvn}$ = PV unit nominal output power.
$\tilde{P}_{PVPPi}$, $\tilde{P}_{WPPi}$ = bus i PVPP and WPP power generations.
$\tilde{Q}_{ci}$ = bus i SVC.
$\tilde{Q}_{Di}$, $\tilde{Q}_{Gi}$ = bus i reactive power demand and generation.
R_c = certain irradiance point.
S = PV module surface solar irradiance.
S_{stc} = standard test conditions solar irradiance.
$\tilde{T}_i$ = transformer tap-change position.
TSC , TSC_{max} , TSC_{min} = total system cost and its maximum and minimum value.
$\tilde{\boldsymbol{u}}$ = set of control variables.

[1]*School of Electrical Engineering, Institute of Engineering, Suranaree University of Technology, Nakhon Ratchasima, Thailand.*
**Corresponding author:* Keerati Chayakulkheeree; Email: keerati.ch@sut.ac.th.

v = wind speed.

v_n, v_{ci}, v_{co} = wind nominal, cut-in, and cut-out speeds.

VMD, VMD_{max} VMD_{min} = voltage magnitude deviation, and its maximum and minimum value.

$\tilde{\boldsymbol{x}}$ = set of dependent variables.

$\tilde{\theta}_{ij}$ = buses i and j voltage angles.

λ_{APL}, λ_{TSC}, and λ_{VMD} = satisfaction function of real power loss, total system cost, and voltage magnitude deviation.

λ_T = overall satisfaction function.

Denote

~ = probabilistic value.

L = lower or minimum limit.

U = upper or maximum limit.

1. INTRODUCTION

Since its introduction nearly fifty years ago, optimal power flow (OPF) has continued to attract substantial attention in power system research. According to [1, 2], the OPF model uses a difficult and non-convex optimization procedure to find the best power system solution while taking safety considerations into account. The main aim of the OPF formulation is to obtain the ideal power system operating conditions depending on the desired result. The OPF then chooses the best values for the control variables. As indicated in [3], the OPF problem also addresses the requirement to uphold power balance and abide by functional limitations inside the system. The OPF solution ensures that the electrical system functions efficiently, complies with equipment operating constraints, satisfies power flow equations, and supports electrical system safety by modifying the network settings, as shown in [4].

It is referred to as a multi-objective problem when the OPF problem comprises more than one objective functions [5], subject to a set of operational equality and inequality constraints. In optimization processes, multi-objective optimization is essential. Traditionally, numerous objectives are combined into a single purpose to solve these issues. In this procedure, conflicting objectives are defined as multi-objective optimization and are then represented by either a fuzzy decision-making methodology [8, 9] or the Pareto fronts optimal method [6, 7]. When one objective cannot be improved without compromising another, the Pareto fronts can be used to determine the best course of action. As an alternative, the fuzzy decision-making approach is utilized to identify the optimal deal option for the trade-off front, where several competing objectives coexist.

Renewable energy sources have received more and more attention recently and have been integrated into the electricity grid. When compared to traditional thermal units, these clean energy solutions have proven to be quite advantageous [10]. However, the inherent unpredictability of solar irradiance and wind speed in various places poses a substantial obstacle to the integration of photovoltaic and wind power plants (PVPP and WPP). Additionally, there is ambiguity regarding the system's overall load. Probabilistic load flow must be applied to evaluate PVPP and WPP generator performance in power systems effectively [11]. B. Borkowska [12] was the first to present the idea of probabilistic load flow (PLF) to overcome load uncertainty. Inputs like load uncertainty, wind speed, and solar irradiance must be defined by suitable probability density functions (PDFs) for establishing the state variables to carry out reliable calculations for systems with uncertainty.

Under the emerging high penetration of distributed energy resources condition, the probabilistic optimal power flow (POPF) has received a lot of interest lately since it has proven to be an efficient tool for examining uncertainty in power systems. To identify the ideal solution statistical interval, POPF handles the uncertain variable in the power system by a probability distribution model. In numerous studies, a variety of techniques for performing POPF have been suggested. Analytical POPF approaches [13], the Point estimation method [14], and Monte-Carlo simulation (MCS) are a few examples. The latter is the most often used method. Due to its simplicity and high accuracy, MCS is frequently used to correctly depict the true characteristics of power systems [15]-[28].

In the pertinent literature, several strategies have been proposed, with a particular emphasis on probabilistic load flow (PLF) including PVPP and WPP generators [18]–[21]. Non-linear MCS, linear MCS, convolution-based approaches [25], Markov-based approaches [26], special distribution-based approaches, Bayesian-based approaches, and hybrid approaches are some of the key approaches covered in [27], all of which extend POPF techniques.

Due to their accuracy in describing the characteristics of power generation and demand, stochastic models have recently gained prominence in both operation and planning of power systems. To accurately capture the dynamic behaviors of solar irradiance and wind speed, these models still need to be improved. In this research paper, the practical load profiles of the power system are used to estimate the load probability density function (PDF). The proposed method utilizes a Normal PDF to express the load uncertainty, and interestingly, the uncertainty of solar irradiance is also represented using a Normal PDF, incorporating the load uncertainty as well [29]. While Weibull PDF is commonly used to model wind speed [30], a discrete PDF will be employed in this study to model the output power due to the wind energy conversion system (WECS) [10]. This approach aims to enhance the accuracy of predicting the behavior of wind power generation.

The article emphasizes the importance of total system cost minimization for achieving economic efficiency, benefiting both electricity producers and consumers. Additionally, it highlights the significance of minimizing

losses in determining system efficiency, as losses can negatively impact power transfer efficiency and voltage profile. Moreover, the article emphasizes the importance of voltage magnitude deviation as a key indicator of power supply quality. To address problems with multiple conflicting objectives and numerous decision variables, the article proposes the use of multi-objective optimization. The major contributions of this article are as follows:

- The formulation of the optimal power flow (OPF) with three objective functions for minimization are TSCM, APLM, and VMDM, respectively.
- The primary contribution lies in introducing fuzzy satisfactory functions (FSF) using particle swarm optimization (PSO) to determine the probabilistic multi-objective OPF.
- The method is evaluated through simulations on a adjusted IEEE 30-bus test system, incorporating PVPP and WPP as case studies.

By incorporating these contributions, the paper aims to provide a comprehensive approach for efficiently addressing the challenges posed by multi-objective optimization in both power system planning and operation. The simulations and case study demonstrate the effectiveness and practical applicability of the proposed method in real-world power systems.

The structure of this article is as follows. The problem formulation is covered in Section 2, while PFOPF algorithm is covered in Section 3. Additionally, Section 4 includes illustrations of the simulation findings and discussion. Finally, Section 5 discusses the conclusion.

2. PROBLEM FORMULATION

2.1. PFMOPF Problem Formulation

In this paper, the probabilistic fuzzy multi-objective OPF (PFMOPF) problem can be represented as follows:

$$\text{Minimize} \quad F_i(\tilde{x},\tilde{u}) \text{ , i = 1, 2,…,N}_{obj} \tag{1}$$

$$\text{Subject to:} \quad g(\tilde{x},\tilde{u}) = 0, \tag{2}$$

$$\square(\tilde{x},\tilde{u}) \le 0. \tag{3}$$

In Equation 1, matrix F_i represents the set of objective functions for minimization including TSC, APL, and VMD. Meanwhile, the vector of dependent variables, denoted by $\tilde{\mathbf{x}}$ can be expressed as:

$$\tilde{x} = [\tilde{P}_{G1}, \tilde{V}_{L1} \dots \tilde{V}_{LNL}, \tilde{Q}_{G1} \dots \tilde{Q}_{GNG}, \tilde{Q}_{WPP}, \tilde{Q}_{PVPP}, \tilde{S}_{l1} \dots \tilde{S}_{lNTL}]^T \tag{4}$$

$\tilde{u}$ is the probabilistic control variables vector,

$$\tilde{u} = [\tilde{P}_G, |\tilde{V}_G|, \tilde{T}, \tilde{X}_C]^T . \tag{5}$$

where,

$$\tilde{P}_G = [\tilde{P}_{G2}, \tilde{P}_{G3}, \dots, \tilde{P}_{GNG}]_{1\times(NG-1)}, \tag{6}$$

$$|\tilde{V}_G| = [|\tilde{V}_{G1}|, |\tilde{V}_{G2}|, \dots, |\tilde{V}_{GNG}|]_{1\times NG}, \tag{7}$$

$$\tilde{T} = [\tilde{T}_1, \dots, \tilde{T}_{NT}]_{1\times NT}, \tag{8}$$

$$\tilde{X}_C = [\tilde{X}_{C1}, \dots, \tilde{X}_{CNC}]_{1\times NC}. \tag{9}$$

Note the matrices $\tilde{\mathbf{P}}_{\mathbf{G}}$ and $|\tilde{\mathbf{V}}_{\mathbf{G}}|$ are include power generation and voltage magnitude of PVPP and WPP.

2.2. PFMOPF

In this article, the following objective functions are considered: TSCM, APLM, VMDM, and multi-objective functions. These objectives are subject to the power balance equations and the system constraints. The aim is to optimize the power system by simultaneously achieving these objectives while satisfying the physical laws represented by the power flow equations and adhering to the operational constraints imposed by the system.

2.2.1. TSCM

The TSCM problem aims to save the generation cost of the power system. The objective function can be expressed as below:

$$\min_u F_1(\tilde{x},\tilde{u}) = \min_u TSC(\tilde{x},\tilde{u}) \tag{10}$$

where,

$$TSC(\tilde{x},\tilde{u}) = \sum_{i=1}^{NG}(a_i + b_i\tilde{P}_{Gi} + c_i\tilde{P}_{Gi}^2) \tag{11}$$

2.2.2. APLM

The APLM aims at the transmission loss minimization as:

$$\min_u F_2(\tilde{x},\tilde{u}) = \min_u APL(\tilde{x},\tilde{u}) \tag{12}$$

where,

$$APL(\tilde{x},\tilde{u}) = \sum_{L=1}^{NTL} g_{L,ij}\left[\tilde{V}_i^2 + \tilde{V}_j^2 - 2\tilde{V}_i\tilde{V}_j\,\widetilde{cos\,\theta}_{ij}\right] \tag{13}$$

2.2.3. VMDM

By keeping the voltage within a specific range, VMDM aims to maintain the voltage quality and stability of the power system. A reference voltage magnitude ($\tilde{V}_i^{ref}$) is commonly set to 1 per unit (1 p.u.) as a target value to do this. The following formulation represents the objective function for VMDM:

$$\min F_3(\tilde{x},\tilde{u}) = \min_u VMD(\tilde{x},\tilde{u}) \tag{14}$$

where,

$$VMD(\tilde{x},\tilde{u}) = \sum_{i=1}^{NL}\left|\tilde{V}_i - \tilde{V}_i^{ref}\right| \tag{15}$$

2.2.4. Fuzzy Multi-Objective OPF Formulation (FMOPF)

Based on a fuzzy trade-off concept, the PFMOPF problem is all together solved for the best TSCM, APLM, and VMDM solution.

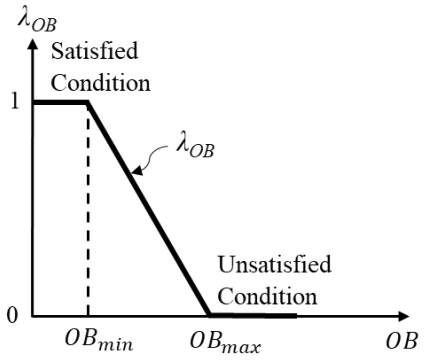

Fig. 1. FSF of OB.

The fuzzy multi-objective optimization technique formulates the fuzzy satisfaction for individual objectives [31]. In this way, the multi-objective optimization problem can be resolved compromising all objectives.

$$\lambda_{OB}=\begin{cases}1 & \text{, for } OB \le OB_{\min}\\ \dfrac{-1}{OB_{\max}-OB_{\min}}\cdot OB & \\ +\dfrac{OB_{\max}}{OB_{\max}-OB_{\min}} & \text{, for } OB_{\min} \le OB < OB_{\max}\\ 0 & \text{, for } OB \ge OB_{\max}\end{cases} \quad (16)$$

$$\text{Maximize } \lambda_T = \min\left\{\lambda_{TSC}, \lambda_{APL}, \lambda_{VMD}\right\} \quad (17)$$

The objective function in Equation 16 is used to form the FSF as shown in Figure 1 and Equation 16, where *OB* denotes the individual objective (TSCM, APLM, and VMDM).

The concept of FSFs for TSCM, APLM, and VMDM is the same as in [32].

2.3. Operating constraints

2.3.1. Power balance constraints

The objective functions discussed above must be solved considering the following power balance constraints,

$$\tilde{P}_{Gi} + \tilde{P}_{PVi} + \tilde{P}_{WTi} - \tilde{P}_{Di} = \sum_{j=1}^{NB}\left[G_{ij}\left|\tilde{V}_i\right|\left|\tilde{V}_j\right| cos\left(\tilde{\theta}_{ij}\right) + B_{ij}\left|\tilde{V}_i\right|\left|\tilde{V}_j\right| sin\left(\tilde{\theta}_{ij}\right)\right], \quad (18)$$

$$\tilde{Q}_{Gi} - \tilde{Q}_{Di} = \sum_{j=1}^{NB}\left[G_{ij}\left|\tilde{V}_i\right|\left|\tilde{V}_j\right| sin\left(\tilde{\theta}_{ij}\right) - B_{ij}\left|\tilde{V}_i\right|\left|\tilde{V}_j\right| cos\left(\tilde{\theta}_{ij}\right)\right], \; i=1,\ldots,NB. \quad (19)$$

2.3.2. Operating constraints

According to Equations 20 to 22, the generator constraints are the limits on the voltage that generators can produce as well as their operating levels of real and reactive power at the *i*th bus. Limits for transformer tap-changing and establishing the SVCs can be found in Equations 23 and 24, respectively. whereas the bus voltage magnitude limit, as well as the loading limits for the transmission lines and transformers, are examples of network operational limit limitations as shown in Equations 25 and 26, respectively.

$$|V_{Gi}|^L \le |\tilde{V}_{Gi}| \le |V_{Gi}|^U, \; i = 1, 2,\ldots,NG, \quad (20)$$

$$P_{Gi}^L \le \tilde{P}_{Gi} \le P_{Gi}^U \;, \; i = 1, 2,\ldots,NG, \quad (21)$$

$$Q_{Gi}^L \le \tilde{Q}_{Gi} \le Q_{Gi}^U \;, \; i = 1, 2,\ldots,NG, \quad (22)$$

$$T_i^L \le \tilde{T}_i \le T_i^U \;, \; i = 1, 2,\ldots,NT, \quad (23)$$

$$Q_{ci}^L \le \tilde{Q}_{ci} \le Q_{ci}^U, \; i = 1, 2,\ldots,NC, \quad (24)$$

$$|V_{Li}|^L \le |\tilde{V}_{Li}| \le |V_{Li}|^U, \; i = 1, 2,\ldots,NPQ, \quad (25)$$

$$|MVA_{Li}| \le M\tilde{V}A_{Li}^U \;, \; i = 1, 2,\ldots,NL. \quad (26)$$

3. PFOPF ALGORITHM

MCS, as a well-established numerical method, is used to handle probability-related problems. In the context of the proposed method, MCS is employed to calculate the probabilistic multi-objective OPF. The procedure for implementing the MCS concept can be defined as follows:

Initial power flow solution.
$PGT_{AV}^0 = 0$.
$DPGT = 1$.
$\varepsilon = 0.001$.
MaxIter = 1000.
k = 1.
if $DPGT > \varepsilon$ and k < MaxIter
  Obtain $\tilde{P}_{PVPPi}$ and $\tilde{P}_{WPP}$ by MCS.
  Solve Equation 10, 12, and 14 using PSO.
  Obtain APL_{max}, APL_{min}, TSC_{max}, TSC_{min}, VMD_{max}, and VMD_{min}.
  Define individual satisfying function.
  Compute λ_{APL}, λ_{TSC}, and λ_{VMD}.
  Compute λ_T.
  Compute PGT_{AV}^k.
  $DPGT = \left|PGT_{AV}^k - PGT_{AV}^{k-1}\right|$
  $k = k+1$.
end

The generation from PVPP, WPP, and load demand are all considered as uncertain variables in the suggested strategy. Probability distributions are used to illustrate the variables' inherent uncertainty. Specifically:

3.1. PVPP Output Model

Solar radiation is thought to follow a normal distribution probability theory in the proposed strategy. A continuous probability distribution called a normal distribution defines the likelihood that a continuous random variable will take on a range of values. A normal logarithm distribution describes the normal distribution. The PVPP output power used in this study is regarded as intermittent and uncertain, which

denotes that it can fluctuate erratically over time. A significant component affecting the power generation from PVPP is solar irradiance, which is used to describe the output power of the PVPP as a continuous random variable [33]. In summary, the suggested approach uses a normal distribution to describe solar radiation, and the output power of the PVPP is treated as a continuous random variable based on solar irradiance. This method enables an examination of the PVPP's performance that considers the inherent uncertainties in solar energy production, as follows:

$$\tilde{P}_{PVPPi}(S) = \begin{cases} \tilde{P}_{pvn}\frac{S^2}{S_{stc}R_c} & \text{for } S < R_c \quad \text{,for bus i} \\ \tilde{P}_{pvn}\frac{S}{S_{stc}} & \text{for } S \geq R_c \quad \text{,for bus i} \end{cases} \tag{27}$$

The probability of solar irradiance (S) following normal PDF is defined in Equations 28.

$$f_S(S) = \frac{1}{\sigma\sqrt{2\pi}} exp\left\{\frac{-(x-\mu)^2}{2\sigma^2}\right\} \tag{28}$$

3.2. WPP Output model

The EPP power generation is influenced by the variability of wind speed that varied over the time. As a result of the highly variable nature of wind resources, wind speed distributions are commonly characterized by a Weibull distribution [34]. The Weibull PDF is commonly used to model wind speeds as it provides a good fit to the observed data in many wind resource regions. The output power of WPP can be obtained by:

$$\tilde{P}_{WPP}(v) = \begin{cases} 0 & v \leq v_{ci} \\ \frac{v-v_{ci}}{v_n-v_{ci}} & v_{ci} < v \leq v_n \\ P_{wtn} & v_n < v \leq v_{co} \\ 0 & v \geq v_{co} \end{cases} \tag{30}$$

The Weibull distribution describes the likelihood of occurrence of certain wind speeds, which in turn influences the wind power plant's output of power. The suggested method can consider the uncertainty and variability associated of wind energy generation by assessing the output power under various wind speed scenarios based on the Weibull distribution, allowing for more precise and reliable forecasts of WPP performance. Weibull PDF can be formulated as follows:

$$f_v(v) = \frac{k}{c} \cdot \left(\frac{v}{c}\right)^{k-1} \cdot e^{-\left(\frac{v}{c}\right)^k} \tag{31}$$

3.3. Load Model

Probabilistic load modeling (PLM) is an essential component of several probabilistic load flow methods. Like how PVPP and WPP are modeled as continuous random variables, the load in the power system is also treated as a continuous random variable, representing the uncertain electrical power consumption in Thailand.

The total load connected to each bus in the power system can be described probabilistically using a normal distribution. The normal distribution is a common PDF that represents continuous random variables with a bell-shaped curve. The PDF for the normal distribution is as follows:

$$f_{P_d}(P_d) = \frac{1}{\sqrt{(2\pi)\sigma}} \exp\left(-\frac{(P_d-\mu)^2}{2\sigma^2}\right) \tag{32}$$

The load at each bus can be represented by probabilistic model using the normal distribution, capturing its variability and uncertainties. With the use of this PDF, the suggested method can more accurately examine the effects of unpredictable energy consumption on the power system while also increasing the accuracy of the load flow analysis and enhancing system performance under varied load situations.

4. SIMULATION RESULT AND DISCUSSION

The PFMOPF simulation is conducted on an adjusted version of the IEEE 30-bus test system, that includes the integration of PVPP, WPP, and load. The results of TSCM, APLM, VMDM, and multi-objective OPF, are addressed and discussed. Figure 2 illustrates the configuration of the adjusted IEEE 30-bus test system including the connection of PVPP and WPP. The system data required for the simulation is obtained from a reliable source, referenced as [35]. This data includes the technical specifications, characteristics, and parameters of the PVPP, WPP, and load elements integrated into the system.

In the proposed approach, the renewable energy sources: WPP and PVPP generator are added to the IEEE 30-bus system. The model accounts for the load demand uncertainty, which is modeled as a PDF. A MCS is run repeatedly until the average total power generation converges close to the previous iteration to handle the uncertainty related to renewable energy generation and load demand. In Figure 3, the results of the MCS are presented. The mean value (μ) of the solar irradiance is determined to be 0.7805, while the variance (σ) is calculated to be 0.0242. These values are crucial for accurately characterizing the solar irradiance as a continuous random variable in the probabilistic modeling. The PVPP rated power connected to bus 30 is specified to be 25 MW, as obtained from the relevant source [35]. This rated power value is used to determine the capacity and performance of the PVPP within the power system.

In this article, the wind speed PDF is represented using a Weibull distribution [34]. The Weibull PDF is a flexible continuous probability distribution that can be various shapes depending on the values of its parameters. The wind speed for the WPP connected at bus 19 is modeled using Weibull PDF. The PDF is characterized by the scale factor 'c' and the shape factor 'k'. The scale factor 'c' determines the location of the distribution, while the shape factor 'k' determines the shape of the distribution. The specific values for v_n , v_{ci}, v_{co}, are 10, 2.7, and 25 m/s, respectively.

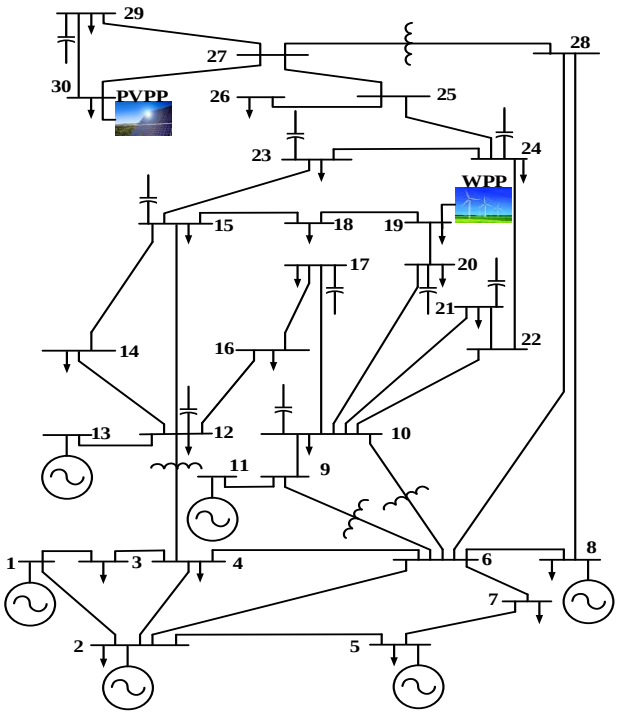

Fig. 2. The adjusted IEEE 30-bus test system.

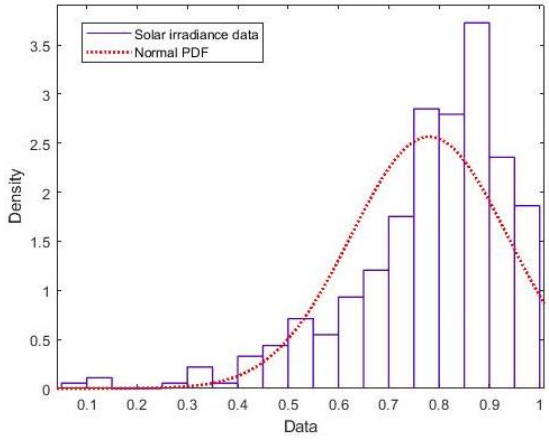

Fig. 3. The PDF of solar irradiance data.

The normalized wind speed is estimated by the Weibull distribution with the following values:

Scale factor 'c': 0.493 and

Shape factor 'k': 2.459.

Figure 4 displays the representation of the Weibull distribution with the given parameters, illustrating how the wind speed probabilities are distributed across different wind speed values.

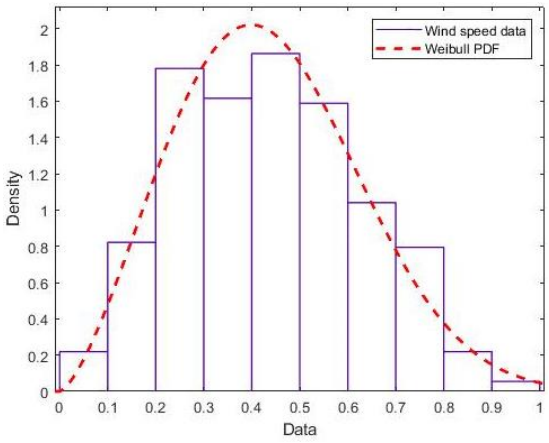

Fig. 4. The PDF of wind speed.

Table 1. The results of PFMOPF

Control Variables	Mean	S.D.
P_{Gi} (MW)		
2	38.868	7.449
5	31.338	5.238
8	23.779	7.414
11	19.010	5.348
13	17.874	5.190
$\|V_i\|$ (p.u.)		
1	1.036	0.032
2	1.029	0.032
5	1.013	0.031
8	1.022	0.031
11	1.011	0.036
13	1.011	0.026
19(WPP)	1.014	0.019
30(PVPP)	1.040	0.020
T_{i-j}		
6-9	1.014	0.055
6-10	1.006	0.067
4-12	1.004	0.042
28-27	1.003	0.038
X_{Ci} (p.u.)		
10	-27.570	14.487
12	-24.442	15.428
15	-36.064	9.614
17	-28.078	10.760
20	-37.298	9.629
21	-21.742	12.649
23	-37.993	8.437
24	-25.489	10.274
29	-40.195	7.344
TSC ($/h.)	**535.123**	**98.046**
APL (p.u.)	**2.523**	**1.896**
VMD (p.u.)	**0.429**	**0.148**
- λ_T of PFMOPF	**0.741**	**0.077**

In Figure 5, the normalized loading characteristic is presented, showing the PDF for the load. The load PDF is typically characterized by a normal distribution, allowing for a more realistic rendering of the probabilistic load

modeling (PLM) by considering daily hourly loading patterns. For this study, the real power of load is assumed by a normal density distribution. The parameters for the normal distribution are as follows:

Mean (μ) = 0.7748 and
SD (σ) = 0.0077.

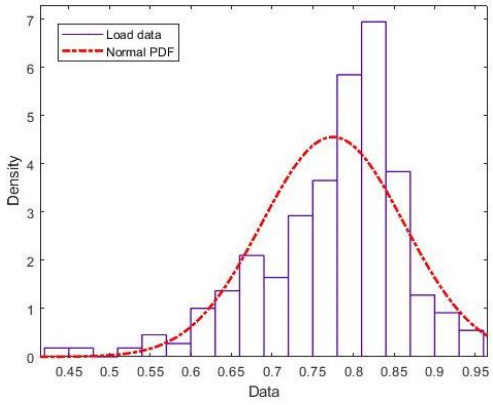

Fig. 5. The PDF of active power load.

The normal distribution with these values characterizes the probability of different active power load levels occurring throughout the day, providing a more accurate representation of the load uncertainty and variability.

The proposed PFMOPF control variables are displayed in Table 1 as well as the PDF that expressed by the mean and standard deviation. As a result, the proposed PFMOPF uses the idea of fuzzy satisfactory functions to attempt to establish a compromise among TSCM, APLM, and VMDM. The suggested PFMOPF produced the following results:

Total System Cost:
Mean: 535.123 $/h
Standard Deviation (S.D.): 98.046 $/h
Active Power Loss:
Mean: 2.523 p.u.
Standard Deviation (S.D.): 1.896 p.u.
Voltage Magnitude Deviation:
Mean: 0.429 p.u.
Standard Deviation (S.D.): 0.148 p.u.
Fuzzy Satisfactory Function (λ_T):
Mean: 0.741
Standard Deviation (S.D.): 0.077

The study uses data on Thailand-specific solar irradiation to determine the photovoltaic power plant's (PVPP) power generating characteristics. Every day, noon is the dispatch hour chosen for PVPP operation since it is the time of day with the highest solar irradiation, which maximizes the potential energy production from solar panels. The IEEE 30-bus test system's bus 30 is connected to the PVPP.

Like this, NASA's internet database was used to find the wind speed information for the wind power plant (WPP), specifically for Bangkok, Thailand, at noon. It is simpler to evaluate the performance of both renewable energy sources at the same time because this time was chosen to coincide with solar irradiance data. The power system's bus 19 is linked to the WPP. The load characteristic was created using Thailand's load demand data. The load demand is distributed proportionally in the adjusted IEEE 30-bus test system for simulating the local area's power consumption pattern.

The probability density functions (PDFs) of the ideal control variables from the proposed PFMOPF simulation are shown in Figures 6 to 9. Various characteristics relating to renewable energy sources (such PVPP and WPP) and load demand are included in these control variables. The PDFs display the distribution of these variables while accounting for their erratic behavior. On the other hand, Figures 10 to 13 present the PDFs for the objective functions of the PFMOPF, specifically the TSC, APL, VMD, and -λ_T. These PDFs are obtained by performing 2000 sample Monte Carlo simulations (MCS). The MCS involves generating random samples for the uncertain parameters, running the power flow calculations multiple times, and analyzing the statistical distribution of the objective functions' outcomes.

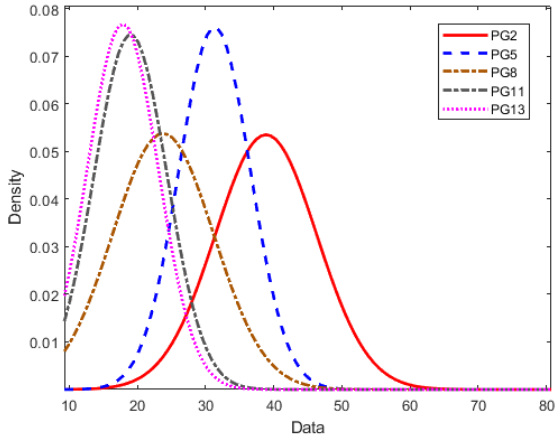

Fig. 6. The generators' output power PDF of PFMOPF.

In this simulation test, the results of the proposed method are compared to the results of individual objective with the 2000 runs of MCS. Figure 14 illustrates the convergence of the MCS results for TSCM, APLM, VMDM, and the proposed PFMOPF. The MCS is considered as a reference method to evaluate the accuracy and effectiveness of the proposed approach. The convergence plot in Figure 14 shows how the objective function values change over successive iterations or runs of the MCS. As the number of iterations increases, the objective function values tend to stabilize and approach a consistent result. This convergence analysis is essential in assessing the reliability of the proposed method and its ability to provide accurate and consistent solutions.

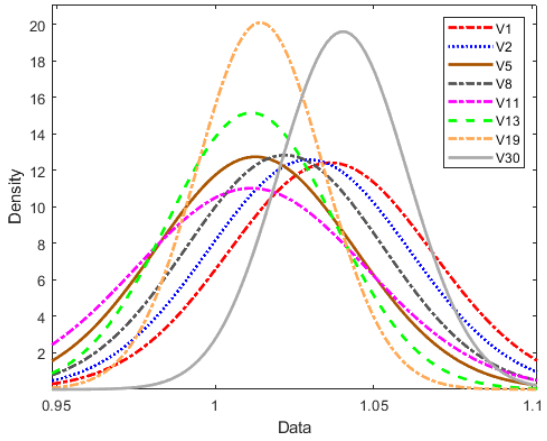

Fig. 7. The generators' voltage magnitude PDF of PFMOPF.

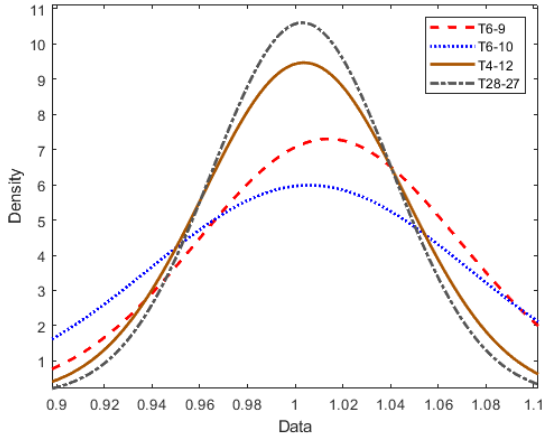

Fig. 8. The Transformer Tap-Changing PDF of PFMOPF.

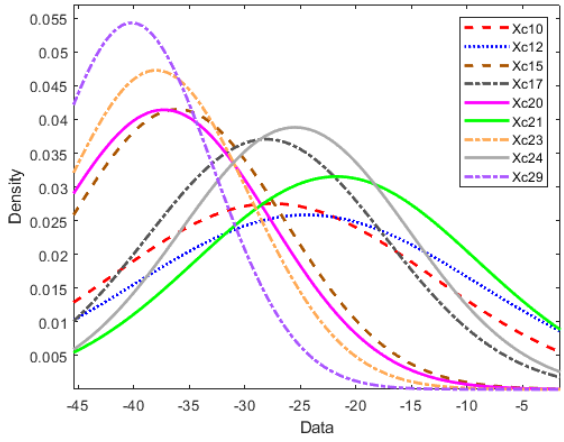

Fig. 9. The SVC Reactance Values PDF of PFMOPF.

By comparing the convergence plots of the proposed method with those obtained from the MCS, researchers can validate the effectiveness of the proposed PFMOPF approach in approximating the true behavior of the power system under uncertainty. If the results from the proposed method closely match the MCS values as the number of iterations increases, it indicates that the proposed approach is a suitable and efficient method for dealing with multi-objective optimization under uncertainty.

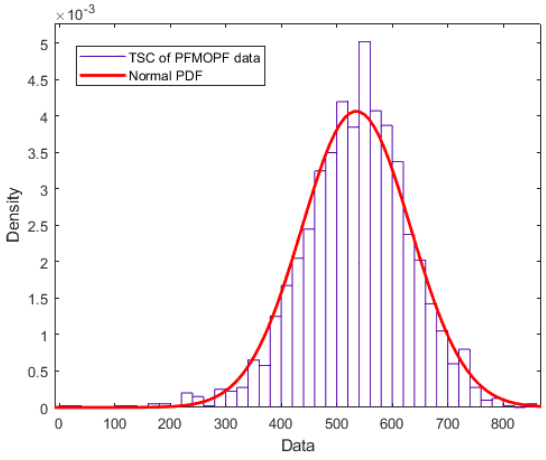

Fig. 10. The TSC PDF of PFMOPF.

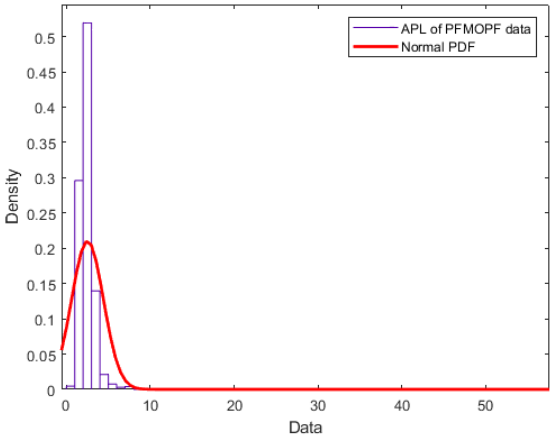

Fig. 11. The APL PDF of PFMOPF.

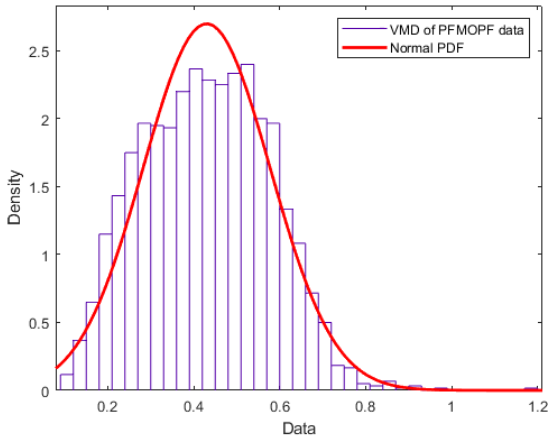

Fig. 12. The VMD PDF of PFMOPF.

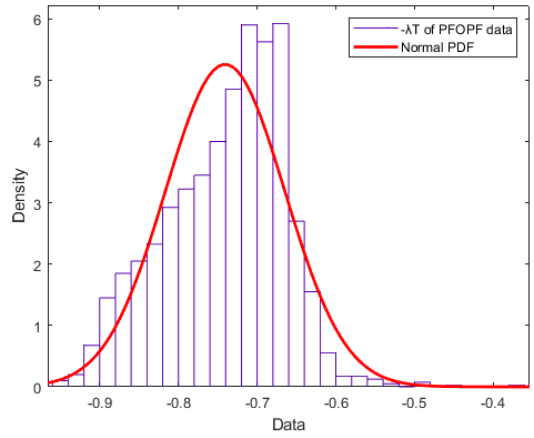

Fig. 13. The Negative Value of λ_T PDF of PFMOPF.

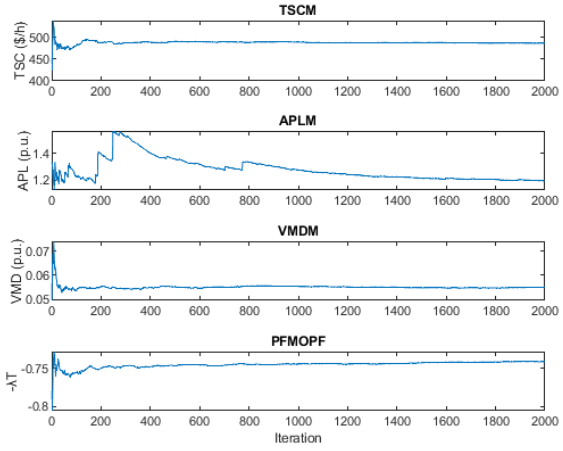

Fig. 14. The convergence of MCS of PFMOPF.

The comparison of convergence plots helps to demonstrate the robustness and reliability of the proposed PFMOPF method, providing valuable insights for future power system planning and operation in a probabilistic environment.

5. CONCLUSIONS

The article proposes a novel approach called PFMOPF, which utilizes various control variables and integrates PVPP, WPP, and load uncertainties using PSO. The method is tested on a modified version of the IEEE 30-bus system. The proposed formulation aims to determine the optimal operating conditions for real power generation, generator voltage magnitudes, transformer tap changes, and SVCs operating values in a probabilistic manner.

The objectives considered in the PFMOPF are TSCM, APLM, and VMDM. These objectives are balanced using a fuzzy concept solution.

The results demonstrate that the PFMOPF can efficiently and effectively minimize individual objective function and maximizes the overall FSF for the purpose of trading among individual objectives. The method successfully incorporates the uncertainties associated with PVPP, WPP, and load of the system, providing robust and reliable solutions.

Possible future research directions in this area include integrating the PFMOPF with other resources, such as demand response, electric vehicle charging, and hydropower generation. Additionally, further verification of the method on larger and more practical power systems would be valuable to assess its scalability and applicability in real-world scenarios. Overall, the proposed PFMOPF method represents a significant contribution to the field of power system optimization under uncertainty and paves the way for exploring more complex and comprehensive solutions in the future.

ACKNOWLEDGEMENTS

This work, Research ID: 2536975, was supported by (i) Suranaree University of Technology (SUT), (ii) Thailand Science Research and Innovation (TSRI), and (iii) National Science, Research, and Innovation Fund (NSRF).

REFERENCES

[1] Bernard C. Lesieutre and Ian A. Hiskens. 2005. Convexity of the Set of Feasible Injections and Revenue Adequacy in FTR Markets. IEEE Transactions on Power Systems 20(4): 1790-1798.

[2] Daniel K. Molzahn. 2018. Identifying and Characterizing Non-Convexities in Feasible Spaces of Optimal Power Flow Problems. IEEE Transactions on circuits and systems 65(5): 672-676.

[3] Dan Wu and Bernard C. Lesieutre. 2018. A Deterministic Method to Identify Multiple Local Extrema for the AC Optimal Power Flow Problem. IEEE Transactions on Power Systems 33(1): 654-668.

[4] Yu-Cheng Chang, Tsung-Ying Lee, Chun-Lung Chen, and Rong-Mow Jan. 2014. Optimal power flow of a wind-thermal generation system. Electrical Power and Energy Systems 55: 312-320.

[5] Mamdouh K. Ahmed, Mohamed H. Osman, Ahmed A. Shehata, and Nikolay V. Korovkin. 2021. A Solution of Optimal Power Flow Problem in Power System Based on Multi Objective Particle Swarm Algorithm. 2021 IEEE Conference of Russian Young Researchers in Electrical and Electronic Engineering (ElConRus).

[6] K. Buayai. 2012. Optimal Multi-type DGs Placement in Primary Distribution System by NSGA-II. Research Journal of Applied Sciences. Engineering and Technology 4(19): 3610-3617.

[7] Wenhua Li, Xingyi Yao, Tao Zhang, Rui Wang, and Ling Wang. 2023. Hierarchy Ranking Method for Multimodal Multi-objective Optimization with Local Pareto Fronts. IEEE Transactions on Evolutionary Computation 27(1): 98-110.

[8] Sundaram B. Pandya and Hitesh R. Jariwala. 2019. Multi-Objective Optimal Power Flow With Improving Voltage Stability and Loss Minimization Using Moth Flame Optimization Algorithm. 2019 IEEE International Conference on Electrical, Computer and Communication Technologies (ICECCT).

[9] K. Chayakulkheeree and W. Ongsakul. 2008. Multi-Objective Optimal Power Flow Considering System Emissions and Fuzzy Constraints. GMSARN International Journal.
[10] John Hetzer and David C. Yu. 2008. An Economic Dispatch Model Incorporating Wind Power. IEEE transactions on energy conversion 23(2): 603-611.
[11] S. Conti and S. Raiti. 2007. Probabilistic load flow using Monte Carlo techniques for distribution networks with photovoltaic generators. Solar Energy 81(12): 1473-1481.
[12] B. R. Prusty and D. Jena. 2017. A critical review on probabilistic load flow studies in uncertainty constrained power systems with photovoltaic generation and a new approach. Renewable and Sustainable Energy Reviews 69: 1286-1302.
[13] A. Schellenberg, W. Rosehart, and J. Aguado. 2005. Introduction to cumulant-based probabilistic optimal power flow (P-OPF). IEEE Transactions on Power Systems 20(2): 1184-1186.
[14] Y. Li, W. Li, W. Yan, J. Yu, and X. Zhao. 2014. Probabilistic Optimal Power Flow Considering Correlations of Wind Speeds Following Different Distributions. IEEE Transactions on Power Systems 29(4): 1847-1854.
[15] C. a. Graham. 2013. Stochastic Simulation and Monte Carlo Methods: Mathematical Foundations of Stochastic Simulation (Stochastic Modelling and Applied Probability).
[16] X. Qing. 2022. Analyzing probabilistic optimal power flow problem by cubature rules. Turkish Journal of Electrical Engineering & Computer Sciences 30(3): 1033-1049.
[17] K.C. Divya and P.S. Nagendra Rao. 2006. Models for wind turbine generating systems and their application in load flow studies. Electric Power Systems Research 76(9-10): 844-856.
[18] Yan Chen, Jinyu Wen, and Shijie Cheng. 2013. Probabilistic Load Flow Method Based on Nataf Transformation and Latin Hypercube Sampling. IEEE transactions on sustainable energy 4(2): 294-301.
[19] F.J. Ruiz-Rodriguez, J.C. Herna´ndez, and F. Jurado. 2012. Probabilistic load flow for radial distribution networks with photovoltaic generators. IET Renewable Power Generation 6(2): 110 –121.
[20] Miao Fan, Vijay Vittal, Gerald T. Heydt, and Raja Ayyanar. 2013. Probabilistic Power Flow Analysis with Generation Dispatch Including Photovoltaic Resources. IEEE Transactions on power systems 28(2): 1797 - 1805.
[21] L. H. Pham, B. H. Dinh, and T. T. Nguyen. 2022. Optimal power flow for an integrated wind-solar-hydro-thermal power system considering uncertainty of wind speed and solar radiation. Neural Computing and Applications 34: 10655-10689.
[22] Mohamed A. M. Shaheen, Zia Ullah, Mohammed H. Qais, Hany M. Hasanien, Kian J. Chua, Marcos Tostado-Véliz, Rania A. Turky, Francisco Jurado, and Mohamed R. Elkadeem. 2022. Solution of Probabilistic Optimal Power Flow Incorporating Renewable Energy Uncertainty Using a Novel Circle Search Algorithm. Energies 15(21).
[23] K. Ramzi and M. Souhil. 2022. Optimal power flow incorporating stochastic wind power using Artificial gorilla troops optimizer. 19th International Multi-Conference on Systems: 2041-2047.
[24] B. Xia, Y. Chen, W. Yang, Q. Chen, X. Wang, and K. Min. 2022. Stochastic Optimal Power Flow for Power Systems Considering Wind Farms Based on the Stochastic Collocation Method. IEEE Access 10: 44023-44032.
[25] N.D. Hatziargyriou, T.S. Karakatsanis, and M. Papadopoulos. 1993. Probabilistic load flow in distribution systems containing dispersed wind power generation. IEEE Transactions on Power Systems 8(1).
[26] W. Sun, M. Zamani, H.T. Zhang, and Y. Li. 2019. Probabilistic Optimal Power Flow with Correlated Wind Power Uncertainty via Markov Chain Quasi-Monte Carlo Sampling. IEEE Transactions on Industrial Informatics 15: 6058-6069.
[27] G. Carpinelli, P. Caramia, and P. Varilone. 2015. Multi-linear monte carlo simulation method for probabilistic load flow of distribution systems with wind and photovoltaic generation systems. Renewable Energy 76: 283-295.
[28] K. Chayakulkheeree. 2013. Probabilistic Optimal Power Flow with Weibull Probability Distribution Function of System Loading Using Percentiles Estimation. Electric Power Components and Systems 41(3): 252-270.
[29] J. Reinders, N.G. Paterakis, J. Morren, and J.G. Slootweg. 2018. A Linearized Probabilistic Load Flow Method to deal with Uncertainties in Transmission Networks. IEEE International Conference on Probabilistic Methods Applied to Power Systems (PMAPS).
[30] Mukund R. Patal. 2006. Wind and Solar Power Systems Design, Analysis, and Operation. Second Edition.
[31] A. D. Richard and M. O. Krzysztof. 2014. Fuzzy Set Theory. ed. Chichester, UK: John Wiley & Sons, Ltd.
[32] P. Muangkhiew and K. Chayakulkheeree. 2022. Multi-objective Optimal Power Flow Using Fuzzy Satisfactory Stochastic Optimization. International Energy Journal 22(3).
[33] Partha P. Biswas, P.N. Suganthan, and Gehan A.J. Amaratunga. 2017. Optimal power flow solutions incorporating stochastic wind and solar power. Energy Conversion and Management 148: 1194-1207.
[34] Imad Abouzahr, and R. Ramkumar. 1991. An approach to assess the performance of utility-interactive wind electric conversion systems", IEEE Transactions on Energy Conversion 6(4): 627-638.
[35] Zia Ullah, Shaorong Wang, and Jinmu Lai. 2019. A Solution to the Optimal Power Flow Problem Considering WT and PV Generation. IEEE Access 7: 46763-46772.